Journal Name

ARTICLE

Well-defined polyelectrolyte and its copolymers by reversible addition fragmentation chain transfer (RAFT) polymerization: Synthesis and applications

Muhammad Mumtaz[1,2], Karim Aissou[1,2], Dimitrios Katsigiannopoulos[1,2], Cyril Brochon[1,2], Eric Cloutet[1,2*] and Georges Hadziioannou[1,2*]

Abstract Reversible Addition-Fragmentation Chain Transfer (RAFT) polymerization of 4-styrenesulfonyl (trifluoromethylsulfonyl) imide potassium salt (SKTFSI) in *N,N*-dimethylformamide (DMF) solution was carried out using 2-(Dodecylsulfanylthiocarbonylsulfanyl)-2-methylpropionic acid (DDMAT) as a reversible chain transfer agent in the presence of 2,2'-azobisisobutyronitrile (AIBN) at 65°C in an inert atmosphere. We showed both homopolymers and well-defined polyelectrolyte diblock copolymer systems could be prepared through the direct polymerization of the charged SKTFSI monomer. To produce Li-ion polyelectrolytes, a cation exchange methodology (*e.g.* $K^+ \rightarrow Li^+$) was used. Self-assembly of single-ion diblock copolymer thin films consisting of a Li-ion conductive PSLiTFSI block associated to a glassy polystyrene block is also demonstrated.

Keywords: RAFT polymerization, polyelectrolyte, block copolymer, self-assembly, thin film.

Introduction

Polyelectrolytes are defined as polymers having pendant ionic functional groups on each repeating unit making these polymers water-soluble. Polyelectrolytes combine both electrolyte and polymer properties since their solutions are electrically conductive, like salts and are often viscous, like polymers. This material is called polyanion if the charge on the polymer is negative or polycation if the charge is positive.[1,2] Polyelectrolytes have been widely used in many applications such as ionic conductors in lithium-ion batteries[3-5], as a dopant and/or stabilizer for the synthesis of semi-conducting polymer dispersions[6-8], as well as to fabricate ambipolar organic transistors[9] or to stabilize magnetite particles[10]. Among anionic polymer, sulfonate constitute the major part of anionic moieties studied so far, mainly due to its easy accessibility via sulfonic acid transformation but there are few examples with sulfonylimide anionic moieties in the literature[11,12]. When considering available and efficient controlled radical polymerization methods, RAFT polymerization is applicable to a wide range of monomers, functional groups, and reaction conditions including aqueous media. The RAFT process is achieved simply by the addition of a suitable Chain Transfer Agent (CTA) to an ordinary radical polymerization system. The homopolymers obtained by the RAFT process can be used as precursors for block copolymers by the addition of a second monomer. From these advantages, many research groups have focused on the use of the RAFT process in the controlled polymerization and the development of macromolecular engineering[13-16]. For instance, Long and co-workers[17] have described the synthesis of PS-*b*-PSLiTFSI-*co*-DEGMEMA-*b*-PS triblock copolymers by RAFT polymerization, which are able to self-assemble into macrophase separated features enabling a substantial improvement of the ionic conductivity. Bouchet *et al.*[18] have reported on the controlled polymerization of SLiTFSI monomer by nitroxide-mediated radical polymerization (NMP) using poly(ethylene oxide) (PEO) as bi-functional macro-initiator. These authors demonstrated PSLiTFSI-*b*-PEO-*b*-PSLiTFSI triblock copolymers combine an excellent Li-ion conductivity with markedly improved mechanical properties although their macrophase separation was not-evidenced. More recently, Inceoglu *et al.*[19] showed that ordered macrophase-separated PEO-*b*-PSLiTFSI electrolytes are less conductive than equivalent disordered electrolytes wherein PEO and PSLiTFSI blocks are intimately mixed.

In this paper, we report on the controlled radical polymerization of KSTFSI monomer and its copolymerization with other methacrylic- and styrenic-based monomers. Especially, we designed a single-ion diblock copolymer consisting of conductive PSLiTFSI block, enabling a high dissociation level due to the weak interaction between Li^+ and TFSI anion, associated to PS block which can insure the mechanical integrity in battery application. Ordered cylindrical and lamellar morphologies produced from solvent-annealed PS-*b*-PSLiTFSI thin films are shown. Nanostructured sub-100 nm polyelectrolyte thin films can be used to envision the design of nanobatteries which meet with the power requirements of devices such as MEMS needing power sources integrated on chip (*i.e.* with the same dimensional scale).[20,21]

Results and Discussions

Single-ion polyelectrolytes described in this work were prepared by using the 4-styrenesulfonyl(trifluoromethylsulfonyl) imide potassium (KSTFSI) monomer which consists of a TFSI anion covalently linked on PS-based monomer unit. Polymerization of SKTFSI (see Fig. S1-S4 for the synthesis and characterization of monomer) was performed using 2-(Dodecylsulfanylthiocarbonylsulfanyl)-2-methylpropionic acid as chain transferring agent (CTA) in the presence of AIBN in DMF at 65°C. Synthesis of PSKTFSI is illustrated in Scheme 1 while Table 1 summarized the characteristics of various PSKTFSI samples.

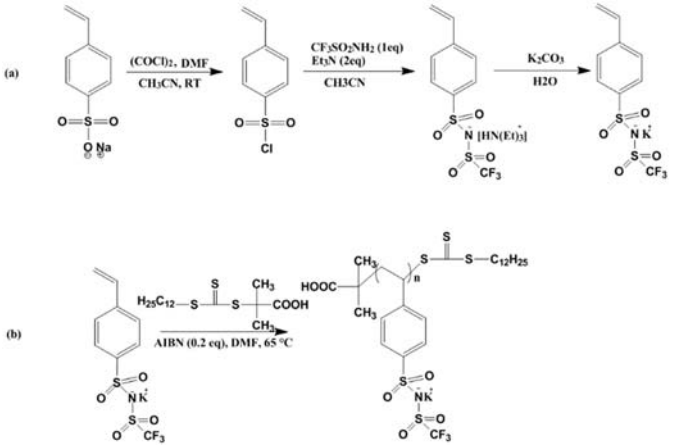

Scheme 1: (a) Synthesis of 4-styrenesulfonyl(trifluoromethylsulfonyl) imide potassium salt. (b) RAFT polymerization of 4-styrenesulfonyl(trifluoromethylsulfonyl) imide potassium salt

Table 1: PSKTFSI homopolymers by controlled radical RAFT polymerization.

Run No.	M/CTA/AIBN	Reaction time (h)	Conversion[a] %	[b]$M_{n\,th}$ g/mol	Mn (SEC) g/mol	[c]M_n (^{1}H NMR) g/mol	[d]M_w/M_n
1	28/1/0.2	2	0.0	nd	nd	nd	nd
2	28/1/0.2	4	15.0	1850	13400	3500	1.05
3	28/1/0.2	5	43.0	4650	15000	5800	1.03
4	28/1/0.2	6	60.0	6350	16200	7400	1.02
5	28/1/0.2	8	75.8	7900	16900	8800	1.02
6	28/1/0.2	9.5	87.4	9100	17500	9900	1.02
7	28/1/0.2	11	92.0	9500	18400	10900	1.02
8	28/1/0.2	14	98.6	10200	19100	12900	1.03
9	14/1/0.2	14	99	5000	10900	6000	1.04
10	57/1/0.2	24	97	20000	30500	nd	1.10
11	113/1/0.2	36	97	40000	58300	nd	1.20
12	227/1/0.2	72	97	80000	73500	nd	1.25
13	282/1/0.2	110	nd	100000	128000	nd	1.70
14	707/1/0.2	192	nd	250000	224000	nd	2.20
15	990/1/0.2	240	nd	350000	220000	nd	2.00

a) Determined by 1H NMR spectroscopy,
b) Theoretical average molar mass: $M_{n\,th}$ = ([SKTFSI]/[CTA] × conv) × M_{SKTFSI} + MCTA, where M_{STFSIK} and MCTA are the molar masses of SKTFSI and CTA, respectively and nd = not determined.
c) Determined by the relative integration of peaks at δ ≈ 7.6 ppm due to phenyl group of PSKTFSI and at δ ≈ 11.9 due to –COOH proton from CTA
d) Determined by SEC using DMF/1% g/L LiBr

To support PSKTFSI polymerization is well-controlled, a set of reactions was performed by keeping initiator/CTA molar ratio at 1/5 and the monomer/CTA ratio such that a theoretical molecular weight of ~10.3 kg/mol at 100 % conversion was expected (runs 1-8, Table 1). All SEC traces are monomodal with no evidence of high molecular weight polymers that may be indicative of uncontrolled polymerization or coupling reactions (Figure 1). Moreover, these SEC traces evidence that the homopolymers produced have a low dispersity (Đ~1.02-1.05). Observed molecular weight, calculated by ^{1}H NMR using the relative integration of peaks at δ ≈ 7.6 ppm due to phenyl group of PSKTFSI and at δ ≈ 11.9 ppm due to –COOH proton from CTA,

are very close to the theoretically calculated molecular weight based on their conversion (Figure 2). However, the molecular weights derived by SEC are different from the ones determined theoretically based on conversion or by ^{1}H NMR spectroscopy. This fact can be explained by the different hydrodynamic volume of the PSKTFSI in comparison with the PS (in DMF/LiBr 1g/L).

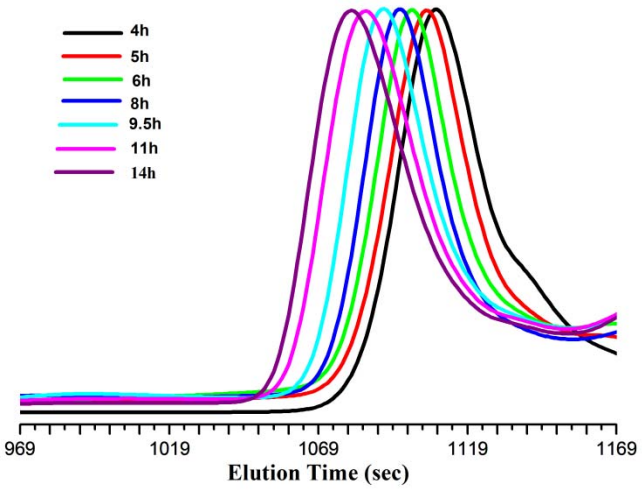

Figure 1: SEC traces for PSTFSIK homopolymers along polymerization time using DMF as an eluent.

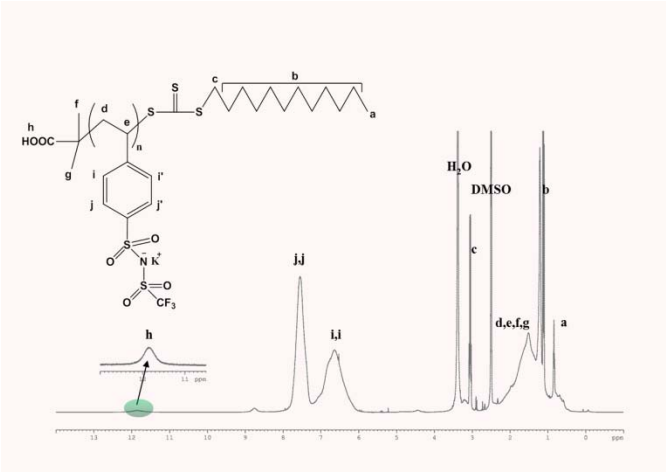

Figure 2: ^{1}H NMR of PSKTFSI homopolymer in DMSO-d_6 (run7, Table 1) at room temperature

To further characterize the controlled/living nature of the chain growth polymerization, different kinetic representations of the experimental results such as conversion of monomer vs time, molecular weight (^{1}H NMR) vs time, M_n, th vs conversion and $\ln[M]_0/[M]$ vs time were plotted (Figure 3). A linear relationship molecular weight (^{1}H NMR) vs time, $M_{n,\ th}$ vs conversion and $\ln[M]_0/[M]$ vs time shows the controlled and living nature of the polymerization and is in accordance with the text books on controlled polymerization. From Table 1 and Figure 3a, it appears that the start of the polymerization is characterized by an induction period (at least up to 2h at 65°C).

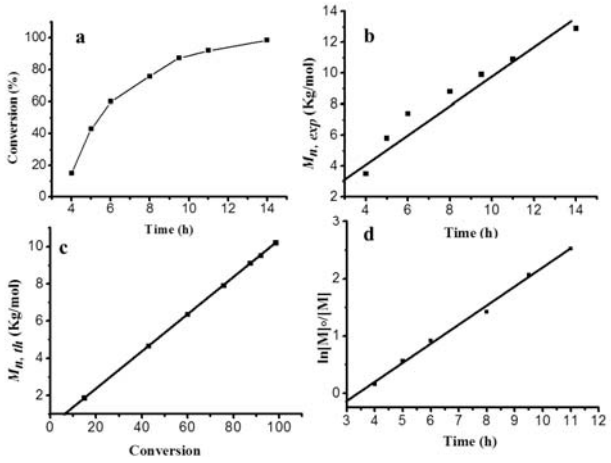

Figure 3: Kinetic plots (a) conversion *vs* time, (b) molecular weight M_n (^{1}H NMR) *vs* time, (c) $M_{n,th}$ *vs* conversion and (d) $\ln[M]_o/[M]$ *vs* time for RAFT polymerization of SKTFSI

Preparation of PSKTFSI polyelectrolytes with high and very high molecular weights were also evaluated (see Table 1, runs 10-16) to show the effectiveness of this polymerization route. In parallel with the growth of the PSKTFSI chain, one can note the increase of the dispersity up to 1.25 for a molecular weight (determined by SEC) of 73.5 kg/mol and even higher (Đ~2.2) for the 224 kg/mol., which could be due to the less available chain end and thus to the presence of dead chains.

Thermal degradation of the PSKTFSI samples was evaluated by thermogravimetric analysis (TGA) performed under air at different heating rates (3 and 5 °C/min) (see Fig. S5). Regardless neither of the molecular weight nor the heating rate, it is obvious that all PSKTFSI samples behave similarly and degrade following different steps. The weight loss occurring from 50°C to 170°C is due to the removal of physically bound water. Afterwards, there are three common noticeable degradations. The first degradation starts at above 370°C and is extended to about 420°C with approximately 12% loss in weight. The second degradation begins above 430°C and is continuous till about 510°C with nearly 25% weight loss. The third and final degradation starts at above 530°C up to about 620°C with approximately 30% loss in weight. For comparison, the lithium salt of the PSTFSI was prepared by ion exchange from already prepared PSKTFSI (run 10, Table 2). PSLiTFSI showed almost similar thermal stability as PSKTFSI with no-change in its stability behavior whether TGA were performed under air or nitrogen which is somewhat different from previously reported data[12,17] (see Fig. S6). The mechanism for the degradation of PSKTFSI and PSLiTFSI is in accordance with the degradation process already reported in the literature for the poly(styrene sulfonate) sodium salt[22].

The thermal behavior of the PSKTFSI samples was studied by differential scanning calorimetry (DSC). For that purpose,

PSKTFSI samples were heated between 0°C to 250°C at the rate of 10°C/min under nitrogen atmosphere. DSC traces for PSKTFSI samples with different molecular weights are shown in Fig. S7. PSKTFSI samples exhibit high Tg values (taken from the second heating run) which increase from 179°C to 239°C as the molecular weight raises from 6 kg/mol to 80 kg/mol.

In order to verify the ability of previously synthesized macro-RAFT agent to give rise to well-defined block copolymers (BCP), we carried out polymerization from PSKTFSI. Results on copolymerization of various methacrylic monomers such as methyl acrylate acid (MAA) and methyl methacrylate (MMA) are summarized in Table 2.

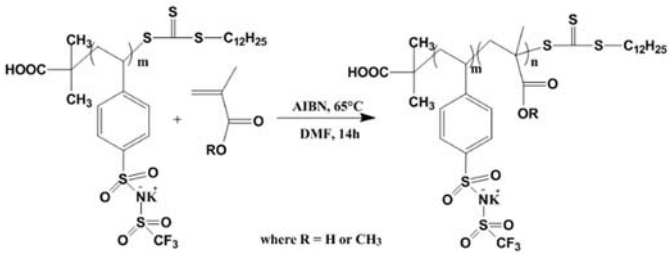

Scheme 2: RAFT synthesis of PSKTFSI-*b*-PMAA, PSKTFSI-*b*-PMMA block copolymers from PSKTFSI macro-RAFT (PSKTFSI-CTA)

Table 2: Characteristics of PSKTFSI -*b*-PMAA and of PSKTFSI-*b*-PMMA block copolymers

Run No.	Macro-RAFT agent	M_n of macro-CTA (g/mol)	2nd monomer	M/CTA/AIBN	Reaction time (h)	Conversion[a]. %	[b]$M_{n\ th}$ g/mol	[c]M_n (^{1}H NMR) g/mol	[d]M_w/M_n
1	PSKTFSI	6000	MAA	67/1/0.2	14	98.0	11800	13000	1.05
2	PSKTFSI	20000	MAA	224/1/0.2	14	97.0	39400	41500	1.08
3	PSKTFSI	10900	MMA	218/1/0.2	14	98.0	32200	29700	1.40

a) Determined by ^{1}H NMR spectroscopy,

b) Theoretical average molar mass: $M_{n\ th}$ = ([SKTFSI]/[CTA] × conv) × M_{SKTFSI} + MCTA, where M_{SKTFSI} and MCTA are the molar masses of STFSIK and CTA respectively.

c) Determined by ^{1}H NMR using first block as a reference.

d) Determined by SEC using DMF as an eluent and polystyrene as standard reference

Molecular weights determined by ^{1}H NMR (using the first block as a reference) were found very close to the predicted values in most of the cases. These results evidence the controlled/living nature of the polymerization method. It is noteworthy that this methodology can give rise to a broad range of macromolecular structures and architectures (e.g. double hydrophilic or hydrophilic-hydrophobic copolymers).

PSKTFSI-*b*-PMAA was prepared using PSKTFSI as a macro-RAFT agent in the presence of AIBN in DMF at 65°C (runs 1-2, Table 2). The 1H NMR of PSKTFSI-*b*-PMAA in DMSO-d6 is shown in Figure 4. The relative integration between –COOH proton of PMAA at 12.3 ppm to the –CH proton of phenyl group of PSTFSIK at 7.6 ppm helped us to calculate the PMAA block molecular weight. Importantly PMAA part of PSKTFSI-*b*-PMAA was not observed when ^{1}H NMR was performed in D2O indicating a sort of micellization of copolymer in which PMAA part is completely trapped inside and cannot be detected.

SEC traces of PSKTFSI-*b*-PMAA block copolymers together with PSKTFSI precursor are shown in Figure 5. The dispersity of block copolymers is quite low with no sign of remaining homopolymer indicating that almost all the polymer chains re-initiate the polymerization of the methacrylic monomer.

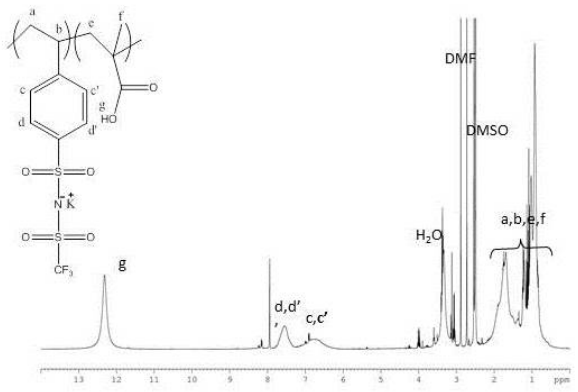

Figure 4:^{1}H NMR of PSKTFSI-*b*-PMAA in DMSO-d6 (run 1, Table 2) at RT.

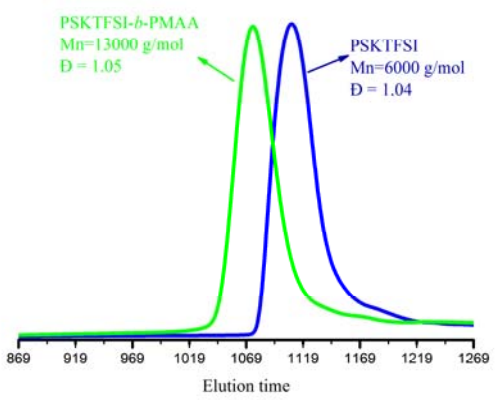

Figure 5: SEC traces of PSKTFSI (run 9, Table 1) and PSKTFSI-*b*-PMAA using DMF as an eluent at 60°C.

Similarly, the PSKTFSI-b-PMMA (run 3, Table 2) block copolymer was prepared using previously prepared PSKTFSI (run 7, Table 1) as a macro-CTA and following similar reaction conditions as above. The ^{1}H NMR of PSTKFSI-*b*-PMMA in the mixture of DMSO-d_6 and $CDCl_3$ (PMMA part was not completely visible when only DMSO-d_6 was used and vice versa) is shown in supporting information (see Fig. S8). In addition, the relative integration of the $COOCH_3$ protons from PMMA at 3.54 ppm versus the –CH protons of phenyl group of the PSTFSIK at 7.6 ppm helped us to determine the molecular weight of the PMMA block.

SEC traces of PSKTFSI homopolymer and PSKTFSI-b-PMMA shown in Fig. S9 indicate that no side reaction has occurred and that the macro-RAFT agent consumption is complete.

Thermal behavior and degradation of the block copolymers were studied by TGA and DSC analysis. TGA traces of PSKTFSI-*b*-PMAA (run 1, Table 2) and PSKTFSI-*b*-PMMA (run 3, Table 2) are shown in Fig. S10. Thermal degradation of PSKTFSI-*b*-PMAA and PSKTFSI-*b*-PMMA follow similar degradation phenomena as the ones observed for their homopolymers 23,24 (see Fig. S11 for illustration).

DSC traces of PSKTFSI-*b*-PMAA and PSKTFSI-*b*-PMMA are shown in Fig. S12-13. For the PSKTFSI-*b*-PMAA, it was not possible to determine any Tg in second heating cycle as PMAA block starts decomposing below 180°C (for illustration please see Fig. S13). In contrast, PMMA block within PSKTFSI-*b*-PMMA system showed higher Tg value than their respective homopolymer of comparative molecular weight (see Fig. S14). The higher PMMA Tg within the BCP system is probably due to some sort of interaction with PSKTFSI block. On the other hand, PSKTFSI in block copolymers showed lower Tg value than its homopolymer with approximately same molecular weight. The lower PSKTFSI Tg is due to the presence PMMA in the block copolymers which act as plasticizers and are responsible for early movement of PSTFSIK chains.

For battery application, nanostructured BCP films are particularly desirable to design lithium conductive solid copolymer electrolyte (SCE) consisting of ionic conductive nanochannels such as lamellae or cylinders surrounded by glassy domains which provide a good mechanical strength over critical Li dendrite growth.[25] To produce microphase-separated SCE, the PS block was combined to different molecular weight PSKTFSI chains so that both cylindrical and lamellar phases were demonstrated. Synthesis of several PS-b-PSLiTFSI systems is now presented.

PSKTFSI macro-RAFT agent was not able to reinitiate the polymerization of styrene in similar conditions as described above. Thus the PS-*b*-PSKTFSI block copolymers were prepared from a polystyrene macro-RAFT agents (see run 1-3, Table 3). First, a PS macro-RAFT agent was synthesized by bulk polymerization of styrene then the growth of the second block of PSKTFSI was achieved in a second step following the same route as described above (scheme 3).

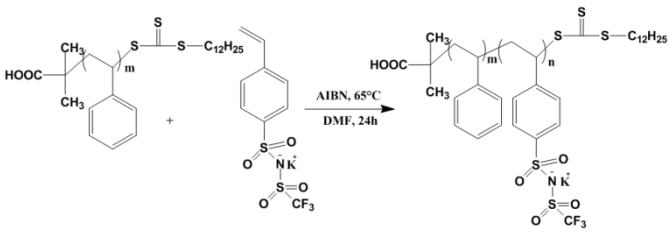

Scheme 3: RAFT synthesis of PS-*b*-PSKTFSI block copolymer from PS-macro-RAFT agent (PS-CTA)

Table 3: Characteristics of PS-*b*-PSTFIK/Li block copolymers

Run No.	Macro-RAFT agent	M_n of macro-CTA (g/mol)	2nd monomer	M/CTA/AIBN	Reaction time (h)	Conversion[a]. %	[b]$M_{n\,th}$ of PS-*b*-PSKTFI g/mol	[c]M_n of PS-*b*-PSKTFI (^{1}H NMR) g/mol	[c]Mn of PS-*b*-PSLiTFI (^{1}H NMR) g/mol	[d]M_w/M_n
1	PS	8800	KSTFSI	19/1/0.2	24	97.0	17300	19390	18430	1.06
2	PS	8800	SKTFSI	58/1/0.2	24	97.0	28700	32900	30700	1.07
3	PS	43000	SKTFSI	122/1/0.2	48	96.0	84700	88500	84400	1.20

a) Determined by ^{1}H NMR spectroscopy,
b) Theoretical average molar mass:$M_{n\,th}$ = ([SKTFSI]/[CTA] × conv) × M_{SKTFSI} + *M*CTA, where M_{SKTFSI} and *M*CTA are the molar masses of STFSIK and CTA respectively.
c) Determined by ^{1}H NMR using first block as a reference.
d) Determined by SEC using DMF as an eluent and polystyrene as standard reference

The ^{1}H NMR of PS-*b*-PSKTFSI (run 1, Table 3) in the mixture of DMSO-d_6 and $CDCl_3$ is shown in supporting information (Fig. S15). The molecular weight of PSKTFSI block was calculated by relative integration between the –CH phenyl protons from PSTFSIK at 7.6 ppm and the sum of the aromatic –CH protons from PS at 7.10 and 6.6 ppm. SEC traces of PS-CTA and PS-*b*-PSKTFSI are shown in supporting information (Fig. S16) indicating also a good control of the polymerization (Mtheo ~ Mexp and low dispersity) and the almost complete consumption of the macro-RAFT agent.

Thermal behavior of the PS-*b*-PSKTFSI copolymer was studied by TGA and DSC analysis. TGA traces of PS-*b*-PSKTFSI (run 1, Table 3) presented in Fig. S10 indicate their thermal behavior shows similar degradation phenomena as the ones observed for their homopolymers[24,26] (Fig. S11). In addition, DSC traces show that PS blocks within PS-*b*-PSKTFSI have also a higher Tg value than its homopolymer of comparative molecular weight (see Fig. S12-S14)

As microphase-separated Li-ion solid copolymer electrolytes are highly desired for battery application, we will now discuss about the phase behavior of PS-b-PSLiTFSI thin films. For that purpose, the PSKTFSI block was first converted into PSLiTFSI by treating different PS-*b*-PSKTFSI systems with $LiClO_4$ salt in ethanol at 60°C. PS-*b*-PSLiTFSI thin films were then spin coated on commercial ITO coated polished glass substrates (RrmsITO = 4.96 nm, Kintec company) from 2 wt% solution of copolymer in THF and their self-assembly was promoted by exposing samples to a continuous stream of vapor produced by bubbling nitrogen gas through liquid consisting of 2:1 v/v THF/water mixture using a set-up similar to the one described previously.[27]

AFM phase images presented in Figure 6 show different solvent-annealed PS-b-PSLiTFSI thin films deposited on ITO substrates. By keeping constant the PS block (9 kg/mol) and varying the PSLiTFSI molecular weight, cylindrical and lamellar domains are produced (Fig. 6a-b). Indeed, in-plane PSLiTFSI cylinders are obtained from solvent-annealed PS_{9k}-*b*-$(PSLiTFSI)_{9k}$ thin films (t ~ 70 nm) with a period, p, around 24 nm while out-of-plane lamellae (p ~ 31 nm, t ~ 40 nm) are produced when the PSLiTFSI molecular weight (20 kg/mol) is increased. The control of the periodicity within the cylindrical phase was also achieved by increasing the PS-*b*-PSLiTFSI molecular weight so that the out-of-plane cylinders with a period of 46 nm were produced from solvent-annealed PS_{40k}-b-$(PSLiTFSI)_{40k}$ thin films (t ~ 60 nm).

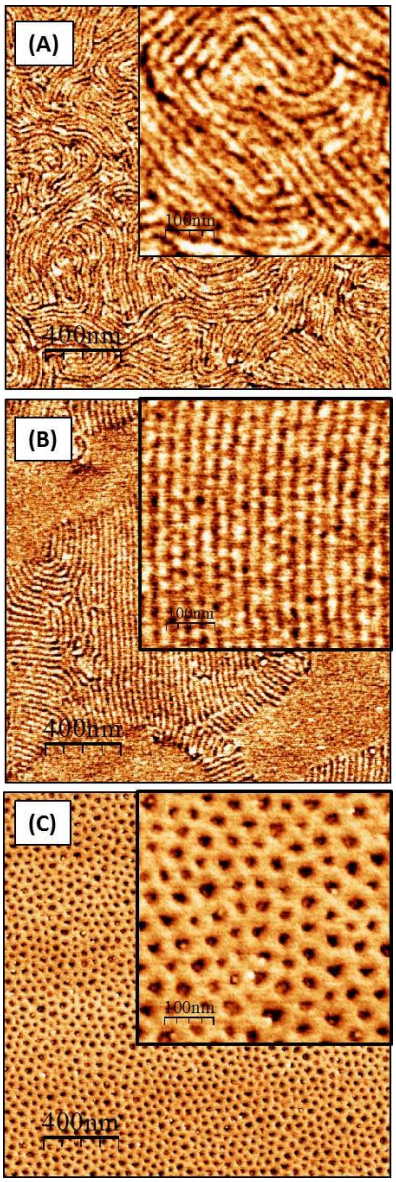

Figure 6: AFM phase views of different solvent-annealed PS-b-PSLiTFSI thin films : (A) PS_{9k}-b-$PSLiTFSI_{9k}$ (t ~ 70 nm, p ~ 24 nm), (B) PS_{9k}-b- $PSLiTFSI_{20k}$ (t ~ 40 nm, p ~ 31 nm) and

(C) PS_{40k}-b- $PSLiTFSI_{40k}$ (t ~ 60 nm, p ~ 46 nm). Inset: magnified corresponding images.

Conclusions

PSKTFSI homopolymers with different molecular weights and a quite low dispersity values were successfully prepared by controlled radical polymerization using RAFT method. Tg of the PSKTFSI homopolymers has been tuned with the polyelectrolyte molecular weight. Self-assembly of sub-100 nm thick solid copolymer electrolytes, consisting of a Li-ion conductive PSLiTFSI block associated to a glassy PS block has also been demonstrated. Out-of-plane PSLiTFSI cylinders and lamellae were produced by tuning the PS-*b*-PSLiTFSI film thickness. We believe these results represent a relevant advance in the design of new single-ion BCP electrolytes for nano-battery application.

Acknowledgements

Authors are grateful to Arkema and to the French Agence Nationale de la Recherche (ANR) for co-funding program "Chaire Industrielle" called 'HOMERIC' (# ANR-13-CHIN-0002-01). This work was also supported by the LabEx AMADEus (ANR-10-LABX-42) in the framework of IdEx Bordeaux (ANR-10-IDEX-03-02), *i.e.* the Investissements d'Avenir programme of the French government managed by the Agence Nationale de la Recherche

Notes and references

1 A. S. Shaplov, P. S. Vlasov, E. I. Lozinskaya, D. O. Ponkratov, I. A. Malyshkina, F. Vidal, O. V. Okatova, G. M. Pavlov, C. Wandrey, A. Bhide, M. Schönhoff, Y. S. Vygodskii, *Macromolecules,* **2011**, *44*, 9792–9803.
2 S. A. Shaplov , R. Marcilla, D. Mecerreyes, *Electrochim. Acta,* **2015**, dx.doi.org/10.1016/j.electacta.2015.03.038.
3 K. Murata, S. Izuchi, Y. Yoshihisa, *Electrochim Acta,* **2000**, *45*, 1501.
4 F. B. Dias, L. Plomp, J. B. J. Veldhuis, *Journal of Power Sources,* **2000**, *88*, 169.
5 H. M. Wolfgang, *Advanced Materials,* **1998**, *10*, 439.
6 F. Louwet, L. Groenendaal,. J. Dhaen, J. Manca,;. J. V. Luppen, E. Verdonck, L. Leenders, *Synth Met.,* **2003**, *135-136*, 115.
7 Qi, Z.; Pickup, P. G. *Chem. Mater*., **1997**, *9*, 2934.
8 X. Sun. M. Hagner, *Macromolecules,* **2007**, *40*, 8537
9 A. Malti, M. Berggren, X. Crispin, *Appl. Phys. Lett*., **2012**, *100*, 183302.
10 P. L. Golas, S. Louie, G. V. Lowry, K. Matyjaszewski, R. D. Tilton, *Langmuir,* **2010**, 26, 16890.
11 A. S. Shaplov, P. S. Vlasov, M. Armand, E. I. Lozinskaya, D. O. Ponkratov,a I. A. Malyshkina, F. Vidal,eO. V. Okatova, G. M. Pavlov, C. Wandrey, I. A. Godovikova,Y. S. Vygodskii, Polym. Chem. 2011, 2, 2609.
12 R. Meziane, J.-P. Bonnet, M. Courty, K. Djellab, M. Armand, *Elecrochimica Acta,* **2011**, *57*, 14-19.
13 B. S. Sumerlin, A. B. Lowe, D. B. Thomas and C. L. McCormick, *Macromolecules*, **2003**, *36*, 1436–1439.
14 B. Ray, Y. Isobe, K. Morioka, S. Habaue, Y. Okamoto,M. Kamigaito and M. Sawamoto, *Macromolecules*, **2003**, *36*, 543–545.
15 M. Arotçaréna, B. Heise, S. Ishaya and A. Laschewsky, *J. Am. Chem. Soc*., **2002**, *124*, 3787–3793.
16 J. F. Lutz, D. Neugebauer and K. Matyjaszewski, *J. Am. Chem. Soc*., **2003**, *125*, 6986–6993.
17 C. Jangu, A. M. Savage, Z. Zhang, A. R. Schultz, L. A. Madsen, F. L. Beyer, T. E. Long, Macromolecules, 2015, 48, 4520-4528.
18 R. Bouchet, S. Maria, R. Meziane, A. Aboulaich, L. Lienafa, J-P. Bonnet, T.N. T. Phan, D. Bertin, D. Gigmes, D. Devaux, R. Denoyel, M. Armand, Nature Materials, **2013**, *12*, 452-457.
19 Inceoglu, S.; Rojas, A. A.; Devaux, D.; Chen, X. C.; Stone, G. M.; Balsara, N. P. *ACS Macro Lett.* **2014**, *3* (6), 510–514.
20 Rhodes, C. P.; Long, J. W.; Doescher, M. S.; Fontanella, J. J.; Rolison, D. R. *J. Phys. Chem. B* **2004**, *108*, 13079– 13087
21 Long, J. W.; Dunn, B.; Rolison, D. R.; White, H. S. *Chem. Rev.* **2004**, 104, 4463– 4492.
22 D.D. Jiang, Q. Yao, M.A. McKinney, C.A. Wilkie, Polym. Degrad. Stabil. 1999, 63, 423.
23 H. G. Schild, *J. Polym.Sci., Polym.Chem*. **1993**, 31, 2403-2405.
24 Q. Zhao, E. T. Samulski, *Polymer*, **2006,** *47*, 663–671.
25 Tatsuma, T.; Taguchi, M.; Oyama, N. *Electrochim. Acta* **2001**, *46* (8), 1201–1205.
26 J. D. Peterson, S. Vyazovkin, C. A. Wight, Macromol. Chem. Phys. **2001**, *202*, 775–784.
27 Gotrik, K. W.; Hannon, A. F.; Son, J. G.; Keller, B.; Alexander-Katz, A.; Ross, C. A. *ACS Nano* **2012**, *6* (9), 8052–8059.